FED-Vol. 176, Bubble Noise and Cavitation Erosion
in Fluid Systems
ASME 1993

CAVITATION EROSION, IMPACT INTENSITY AND PIT SIZE DISTRIBUTION OF JET AND VORTEX CAVITATION

Raynald Simoneau and
Paul Bourdon
Hydro-Québec – IREQ
Varennes, Québec, Canada

M. Farhat and
François Avellan
EPFL–IMHEF
Lausanne, Switzerland

J. M. Dorey
EDF–DER
Chatou, France

ABSTRACT

Three different methods of cavitation erosion measurement are compared and correlated with weight loss rates in two cavitation set-ups: a high pressure cavitation jet producing a high repetition rate of a wide range of impact intensities and a single vortex machine producing a low repetition rate of large collapses. The electrochemical cavitation activated current measurements on pure titanium sensors are calibrated on the jet and used to evaluate erosion rates on the vortex. The cavitation pit counting technique on polished surfaces of 7 different hardness metals is compared with high frequency accelerometer data in both set-ups. Pit dimensions indicate that the impact intensity of the vortex collapses is comparable to that of the lowest intensity of jet cavitation. Good correlations are found between erosion rate, volume pitting rate and high frequency inferred forces over more than 6 orders of magnitude.

INTRODUCTION

Although cavitation erosion in hydraulic systems is a long-standing problem, the damage mechanisms that produce material loss are still poorly understood. It is not yet possible to predict with good accuracy and reliability from the design stage or even from the model tests the actual erosion rate that will prevail on a large prototype hydroturbine or any other large hydraulic machine.

In order to solve that problem, tools that will allow the measurement of the cavitation erosion power of small scale turbine models and correlation with prototype erosion through accurate scaling laws are needed. The results presented in this paper are part of a larger program aimed at developing such tools.

One of the most sensitive and easy techniques to measure cavitation intensity is the high frequency vibratory method with high frequency accelerometers[1,2]. As a counter part of its high sensitivity it suffers from the difficulty of discriminating cavitation against other sources of perturbing noise. It also needs to be calibrated against measured metal erosion rates. It is at this time the best technique to monitor cavitation in both model and prototype machines.

The pit counting technique on polished metal surfaces is also a very sensitive technique that is being developed on a more quantitative basis in the last decade[3,4]. It is more difficult to implement and also needs to be calibrated against metal erosion rate. It has the advantage of indicating the aggressivity and spatial distribution of individual cavitation impacts.

The DECER electrochemical detection technique, developed by Université de Paris in collaboration with Hydro-Québec, provides through the measurement of cavitation activated electrochemical current on titanium sensors an on-line measurement of the instantaneous local erosion rate[5,6]. It is not as sensitive as the two previous methods but it can be used for their calibration in cavitation set-ups where metal weight loss measurements are difficult to achieve such as in a cavitation tunnel[7,8], the vortex machine and small scale turbine models[6,9]. The results obtained with these three techniques will be compared in two different set-ups, a high pressure cavitation jet and the single vortex machine of IMHEF of Lausanne[10]. Table 1 summarizes the different experiments.

Table 1

	JET	VORTEX
Water temperature	10-25 °C	15-25 °C
High pressure	7-35 MPa	100-860 kPa
Low pressure	170-500 kPa	10 -100 kPa
HF acceleration	yes	yes
Pit counting	yes	yes
DECER	yes	yes
Weight loss	yes	no

HIGH PRESSURE CAVITATION JET

Experimental Set-up

The high pressure jet is fed by a high pressure water pump that can deliver up to 40 MPa water to a 0.8 mm sapphire nozzle enclosed in a stainless steel chamber that can sustain pressure up to 1000 kPa. The sapphire nozzle has a conical outlet specially shaped in order to yield the highest cavitation intensity. Both water pressures are controlled by mechanical devices. Water is recirculated with admission of tap water to control pressure and temperature. The test specimen is maintained at a constant distance of 17 mm to the nozzle outlet. Weight losses are measured on dried specimens at appropriate intervals on an electronic balance with 0.1 mg readability. For the pit counting experiments in order to submit the specimen surface to steady state cavitation for a short period of time between 0.03 and 0.15 second, the specimen was mounted on a support rotating at a speed between 10 and 150 rpm.

For the DECER electrochemical detection three different grades of titanium were tested, Ti1, Ti2 and Ti59. The softest high purity Ti59, now available, was used in order to improve the sensitivity of the method. Table 2 lists the materials used either for DECER or pit counting techniques.

Table 2

Identifica.	Hardness	Composition
	Brinell	(w.%)
Al59	16	Al 99.999
Al6061T6	87	Al-0.6Si-1Mg
Cu39	25	Cu 99.95
Ti59-both	55	Ti 99.999
Ti1-DECER	120	Ti 99.1, grade 1
Ti2-DECER	200	Ti 98.9, grade 2
Tig5	350	Ti-6Al-4V, grade 5
316L	130	Austenitic stainless steel
440C	530	Martensitic stainless steel

For the acoustic measurement a high frequency accelerometer, Kistler 8616A1000, was mounted outside the jet chamber on the flange coupling of the rotating shaft of the specimen support assembly.

The DECER calibration

Figure 1 presents the calibration curve for the three grades of pure titanium obtained over the full range of

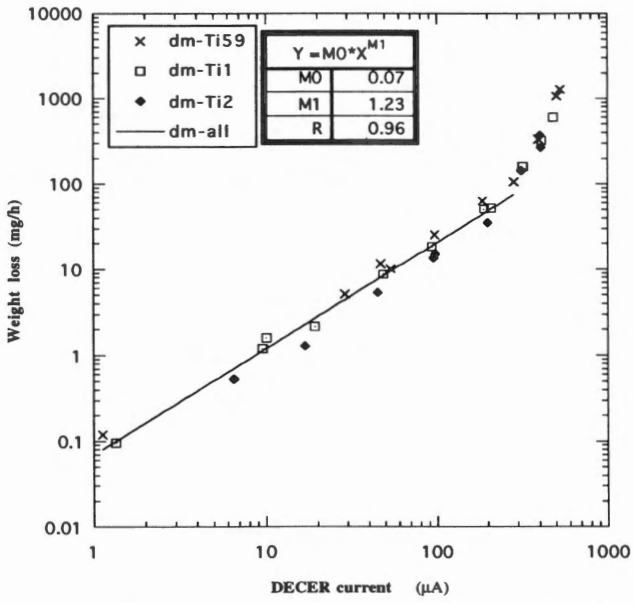

Figure 1. Calibration curve for the three grades of titanium

cavitation intensity of the cavitation jet. In a narrow range of erosion rates a linear relationship is found between the cavitation activated current, I_C, and the erosion rate, dm/dt. In the full range all the points fit well on a single power curve, except for the highest erosion rates where a saturation is observed specially for the softest Ti59. This saturation can be attributed to the fact that the cavitation collapses impact and erode too often the same spot and overlap. The global calibration law is the following:

$$\mathbf{dm/dt\ \ (mg/h) = 0.07 * I_C^{1.23}\ (\mu A)}$$

For the lowest erosion rates the DECER sensitivity can be increased by more than a factor of 3 by using the purest Ti59 instead of the grade 1 Ti.

Pit counting

Samples of the 7 metals or alloys listed in table 2, except Ti1 and Ti2 that were used only for DECER, were prepared in metallographic mounting resin and mechanically fine polished down to 0.05 µm mean roughness. They were exposed to jet cavitation for a short period of time with the help of the rotating support. The cavitation intensity was varied by changing the inlet high pressure. The chamber pressure was adjusted to produce the maximum intensity for each high pressure value. The four test conditions are listed in table 3. The exposed surfaces have the following dimension range: width between 12 and 18 mm and length between 12 and 20 mm. The exposure time was adjusted, trough the rotation speed of the sample holder, in order to have at least 100 pits within the measured surface of 1 cm^2 and less than 25 % of pitted areas in the scanned surface. It was set to 0.15 s for all tests except for the softest metals, Al59, at the highest intensity (35 MPa) for which it was set to 0.03 s.

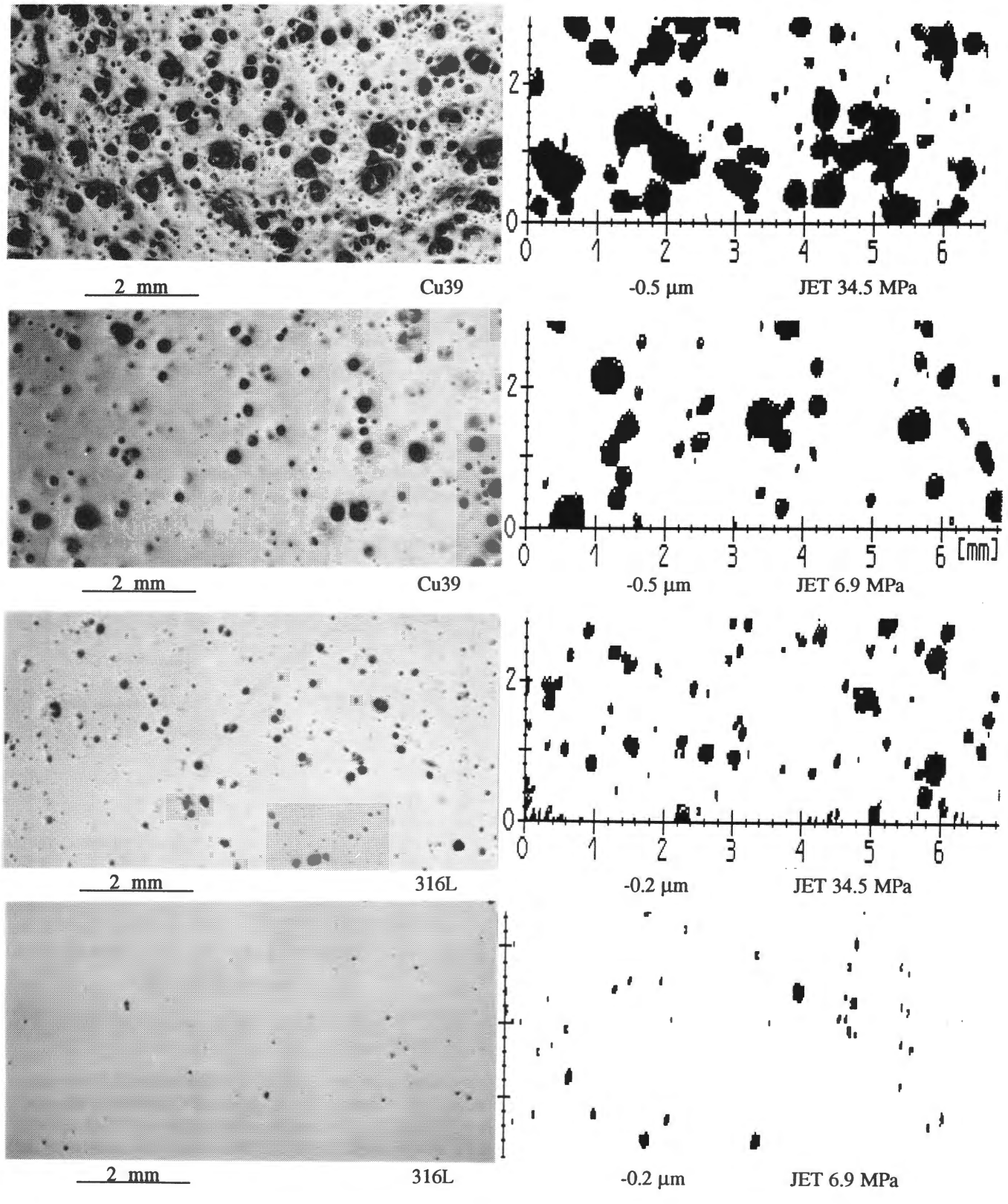

Figure 2. Optical micrographs and pitted area profilometer output taken at a depth of 0.5 µm on Cu39 and 0.2 µm on 316L surfaces exposed to jet cavitation for 0.15 s at 34.5 MPa and 6.9 MPa pressure.

Table 3

Identification	High pressure (MPa)	Chamber pressure (kPa)
7	6.9	169
14	13.8	238
21	20.7	376
34	34.5	513

The pitted surfaces were analyzed with a 3-D optical laser UBM profilometer. With its x-y scanning sample holder this equipment uses a focused laser spot of 1 μm with a z resolution of 5 nm and a x-y resolution of 0.5 μm. The system software can produce 3-D surface plots or contour lines and calculate the total pit area for a given depth. All the samples were scanned on an area of 10 mm by 10 mm at a resolution of 20 points by mm.

Figure 2 compares optical micrographs and pitted area profilometer output of Cu39 and 316L samples exposed at the minimum and maximum jet cavitation intensities. The effect of cavitation intensity and material hardness is obvious. As it can be seen on the micrographs of figure 2 and on the pit diameter distribution of figures 3 and 4, there is a finite number of larger pits characterized by the cavitation intensity and the material hardness, such as about 0.6 mm on Cu39 and 0.2 mm on 316L for the highest intensity. There is also a larger number of smaller pits, of diameter smaller than 0.1 mm. The total number of pits of the order of a few hundreds for an exposure time of 0.15 s corresponds with the characteristic acceleration frequency of a few kHz measured with the high frequency accelerometer.

Figures 5 and 6 present the total pit area calculated at different pit depths for all the materials at the 2 extremum conditions. All the data have been normalized to 100 mm^2 analyzed total area and 0.15 s exposure time. For Al59 at the maximum intensity we had to reduce the exposure time to 0.03 s by increasing the rotation speed by a factor of 5 in order to have an acceptable density of pits. The minimum depth of pits was set at 0.2 μm in order not to include any polishing defect. For an exposure time of 0.15 s the pitted area of the soft Al59 for 34.5 MPa and a depth of 0.2 μm would cover more than the full 100 mm^2 scanned surface. At the maximum intensity, the pitted area at a depth of 0.2 μm goes from 130 % of the exposed surface for the softest aluminum to about 0.3 % for the hardest stainless steel and the maximum pit depth goes from 25 μm to 1 μm. This maximum depth is somewhat reduced for the higher strain hardening metals such as Cu39, Ti59 and 316L. At the lowest intensity no pits were measured at the 0.2 μm depth for the two hardest alloys, Tig5 and 440C.

Figure 7 shows the total volume of pits as calculated from the pitted areas at different depths for all materials and all test conditions. A good correlation is found with the materials hardness. The correlation was not so good with either the materials yield or tensile strength, which is not

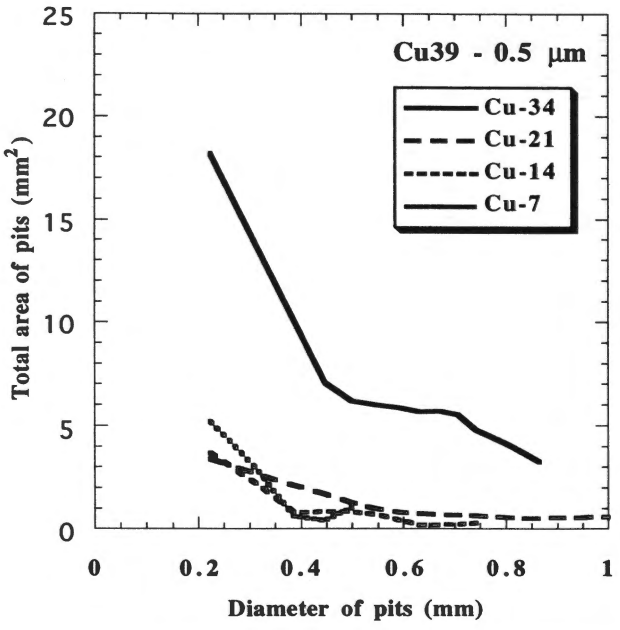

Figure 3. Distribution of pit diameter on Cu39 at the four intensities of the jet as measured at the depth of 0.5 μm.

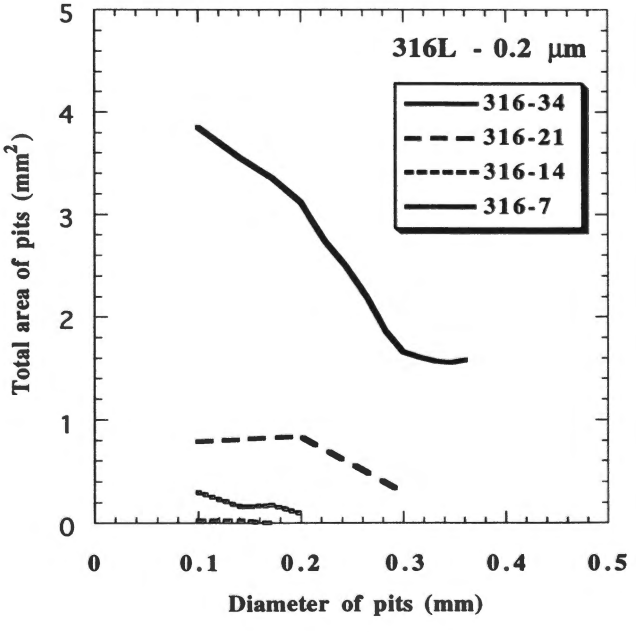

Figure 4. Distribution of pit diameter on 316L at the four intensities of the jet as measured at the depth of 0.2 μm.

surprising since both hardness indentation and cavitation pitting are somehow similar processes, except for the strain rate. These data indicate that strain rate effect is not very important in these materials. There may be some for 316L which presents lower cavitation pitting than predicted by the correlation curve. An opposite effect seems to be prevalent for Al6061T6 and it could be related to the larger brittleness of this hardened alloy.

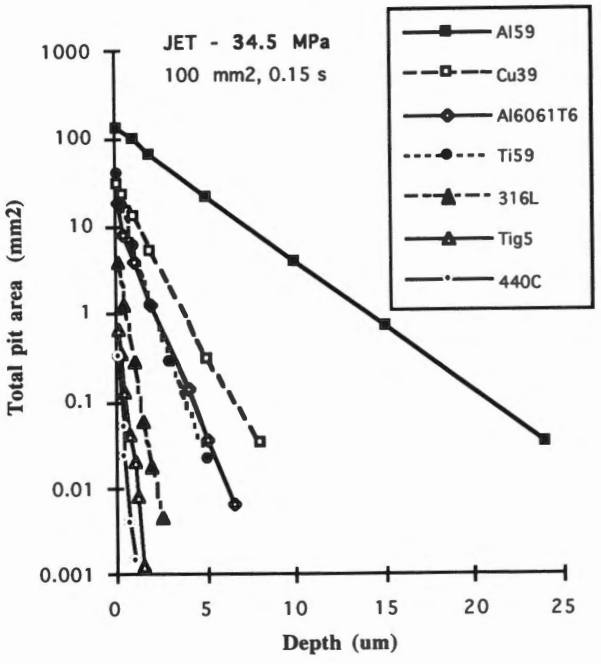

Figure 5. Total pit area and depth for 34.5 MPa jet cavitation

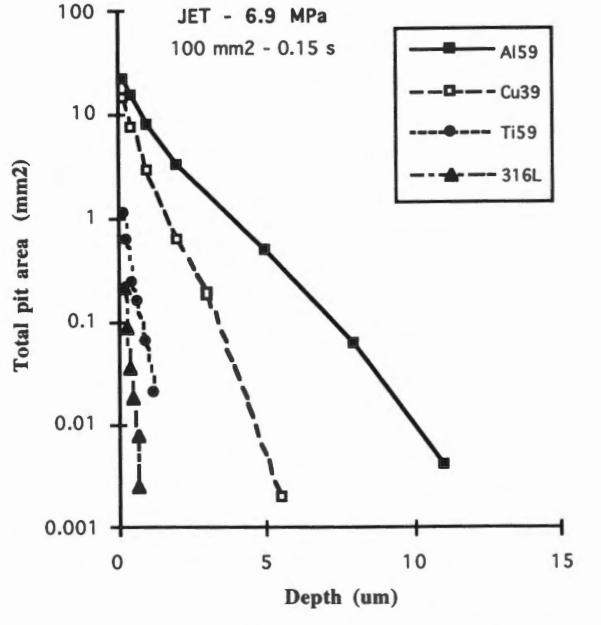

Figure 6. Total pit area and depth for 6.9 MPa jet cavitation

This pit counting technique is good to measure the aggressivity or erosive power of cavitation as it can be seen on figure 8 where the measured steady state (measured after the incubation period) erosion rate of Al6061T6 is taken as a direct measure of erosive cavitation intensity. The results of

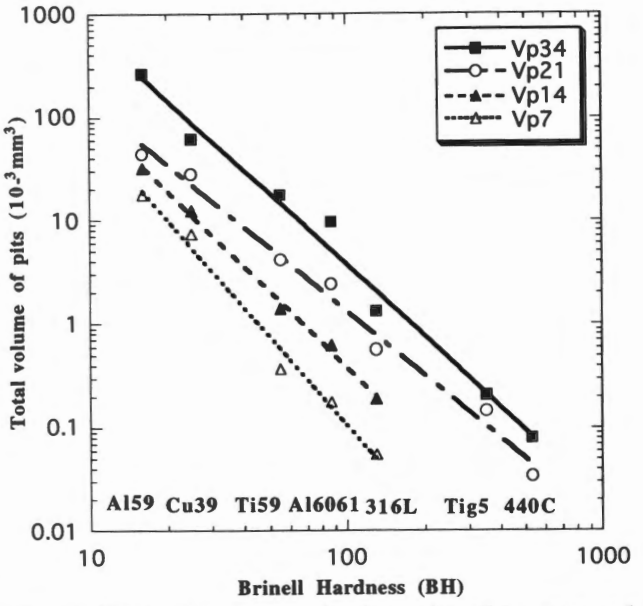

Figure 7. Total pit volume vs hardness for all jet tests and all materials.

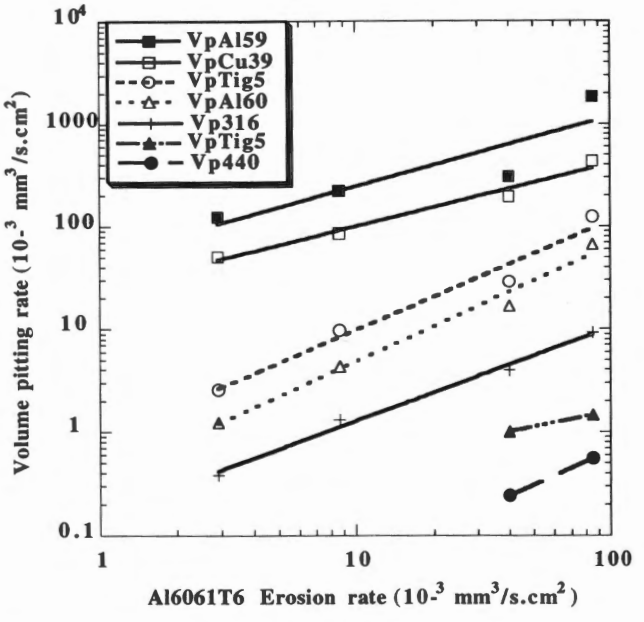

Figure 8. Pitting rate vs Al 6061T6 erosion rate.

the softest Al59 at the two highest cavitation intensities are less good probably because of a saturation effect associated with too long exposure time. The correlation is particularly good for Cu39 and 316L that can be used to cover a fairly wide range of cavitation impact intensity.

The prediction of erosion rate for a given metal from this pit counting technique is not so simple since we have to take into account the intrinsic properties of each metal and alloy, such as the strain hardening, the brittleness and toughness, the oligocyclic fatigue resistance, etc.. This is

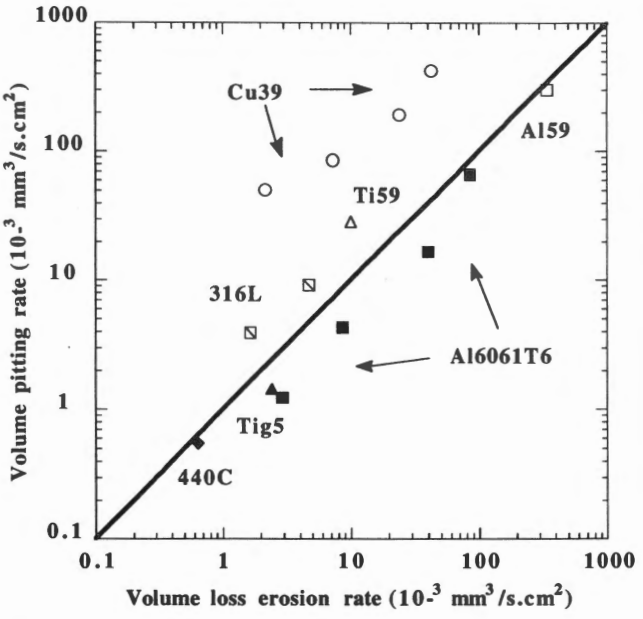

Figure 9. Correlation between the volume pitting rate and the volume loss erosion rate for each metal.

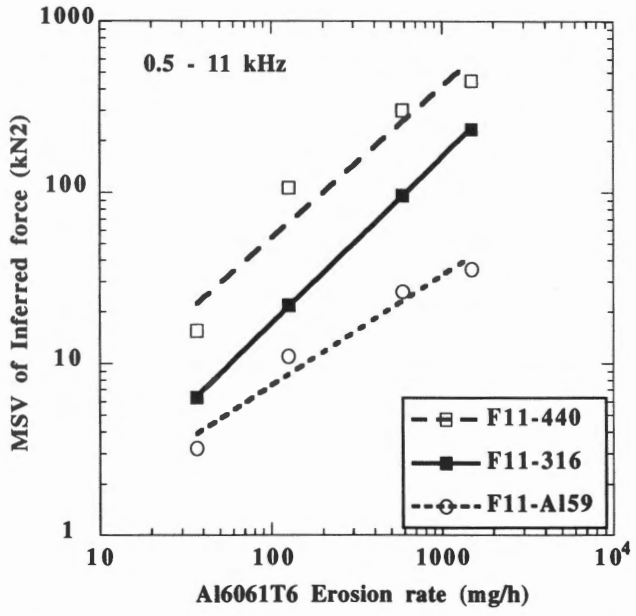

Figure 10. Mean square value of force inferred from accelerometer signal in the 0.5 - 11 kHz bandwidth for 3 hardness metals.

illustrated on figure 9 where we have plotted the volume pitting rate, calculated from the total pit volume, against the volume loss rate calculated from the weight loss rate normalized to the same area (1 cm^2) and time (1 s) as the volume pitting rate. The weight losses have been measured on different samples for longer exposure time in the steady state regime. It can be seen that the more ductile strain hardening and tougher alloys, Cu39, Ti59 and 316L, present a volume pitting rate larger than their volume loss rate and the opposite is observed for the more brittle precipitation hardened alloys, Al6061T6 and Tig5. These data corroborate the observation of brittle fracture observed on the eroded facies of these hardened alloys.

Vibration data

The vibration intensity was measured with the high frequency accelerometer mounted on the external flange of the rotating shaft of the jet cavitation assembly. To verify the effect of the material hardness the measurements were made with the jet impacting three different hardness metals, Al59, 316L and 440C. The mean square value of acceleration was analyzed in three different bandwidths, 0.5 - 11 kHz, 0.5 - 30 kHz and 30 - 50 kHz. The force on the samples was inferred with the help of the transmissibility function measured with an instrumented hammer impacting immersed specimens mounted in the test chamber. Obviously the vibration amplitude was affected by the impacted metal hardness and particularly by a system resonance which was excited strongly at some of the test points. Thus poor correlation was obtained with the MSV of acceleration and the cavitation or erosion intensity. As shown on figure 10 much better correlation was obtained with the inferred force in the 0.5 - 11 kHz bandwidth. Correlation was not as good in the higher frequency bands mainly because of the limited frequency response of the instrumented hammer used for the transmissibility function measurement. Larger forces were however produced on the harder metals. These data illustrate well how caution should be taken in dealing with the acoustic detection of erosive cavitation. One should take into account not only the transmissibility function but also the nature of the metals being eroded. When such precautions are taken the two methods can well measure the erosive power of cavitation as it is illustrated on figure 11. The jet erosive power is measured by the weight loss erosion rate of Al 6061T6 alloy.

VORTEX CAVITATION

Experimental Set-up

The cavitation vortex generator, described in a previous paper[10], produces a repeated expansion and collapse of a large water vapor vortex by water-hammer waves generated by the successive closure and opening of a rotating valve. The cavitation impact intensity can be varied by the flow rate and high pressure of the incoming water, the low pressure at the outlet, the rotation speed of the valve and the air content measured via the O_2 content. For the present tests the end surface of an 11 mm diameter metal cylinder, mounted through the wall of the test section, was exposed to the vortex collapses. For the vibration measurements a high frequency accelerometer BK8309 was threaded to the other end of the 55 mm long metal cylinder. For the electrochemical DECER measurements, titanium grade 1, Ti1, was used and for pit counting, copper, Cu39 and stainless steel, 316L, were taken from the same bar as for

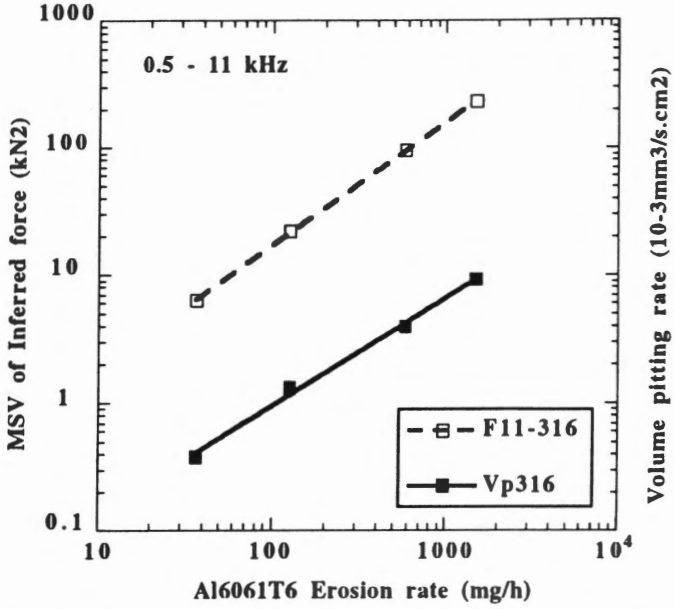

Figure 11. Comparison of the two cavitation detection method data, pit counting and acoustic, obtained on 316L samples at the four intensities of the jet.

the jet tests. Three different impact intensities were used with the conditions shown in table 4.

Table 4.
The 3 tests conditions of vortex cavitation pitting.

Tests		T1	T2	T3
P1	(kPa)	8.4	4.4	2.1
P2	(kPa)	100	50	27
O2	(ppm)	0.7	0.4	0.4
Rotation	(rpm)	200		
Time	(s)	45 - 120		
Temp.	(°C)	19 - 25		

The DECER erosion rate

Figure 12 presents simultaneous time traces of accelerometer and DECER erosion current pulses obtained at the T1 test conditions. The electrochemical current is suddenly excited at the cavitation collapse, indicated by the accelerometer signal, by the erosion and depassivation of the impacted titanium surface which repassivates slowly during the 0.3 s interval between each impact. In order to provide repeatable and calibrated current signals, the surface of the titanium probe had to be pre-incubated by a long exposure (2 days) in the operating vortex. To obtain the average erosion rate as calculated from the calibration curve of figure 1, the current signal was time integrated.

Figure 13 presents results of DECER Ti1 average current together with the MSV of the acceleration signal during a continuous run of three hours of the vortex after original

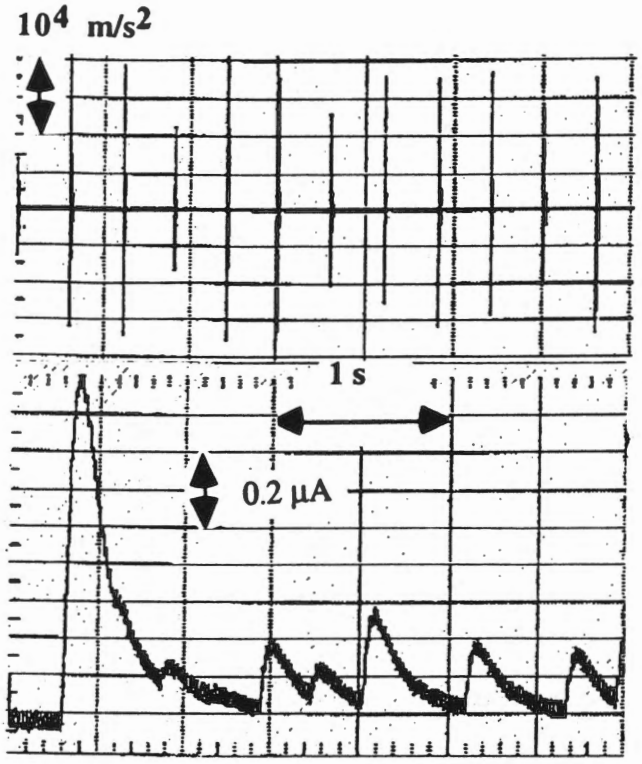

Figure 12. Simultaneous time traces of accelerometer and DECER erosion current pulses obtained at the T1 vortex test conditions.

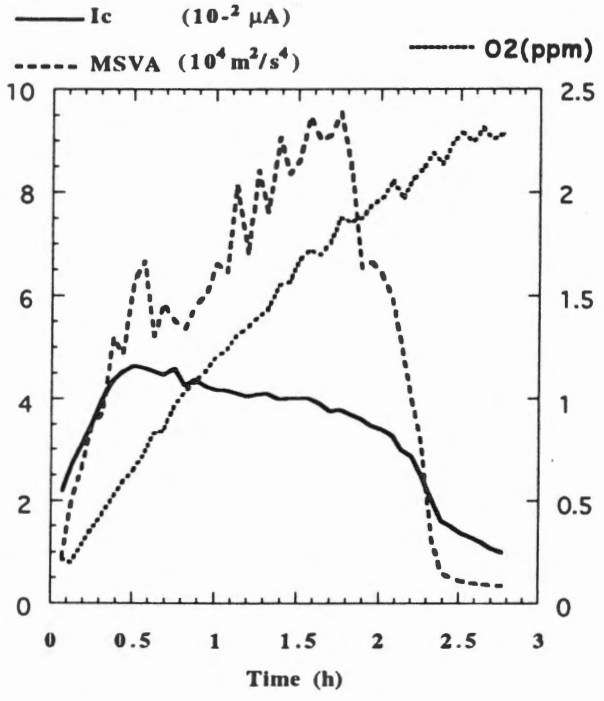

Figure 13. Evolution of O2 content, DECER current, I_C, and mean square value of acceleration during a 3 hour period of vortex operation at the maximum intensity condition, T1.

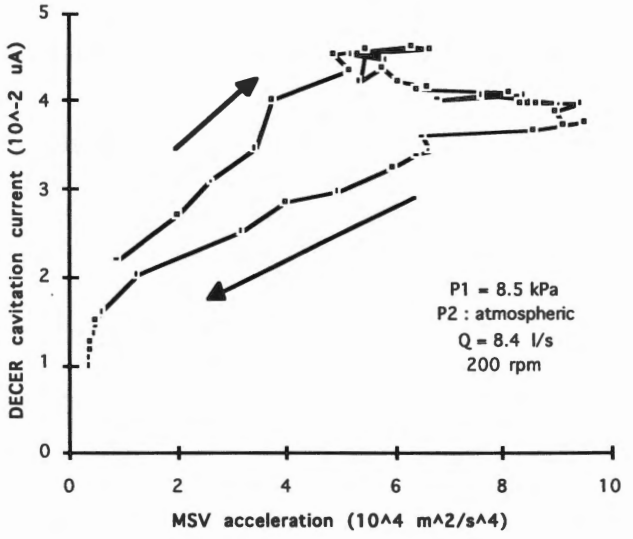

Figure 14. Correlation between erosion DECER current and MSV of acceleration measured during the 3 hour ingassing period.

outgassing. During this period the O_2 content increases slowly from 0.2 to 2.4 ppm. The accelerometer signal is acquired, simultaneously with the DECER current, in the full bandwidth at 1 MHz sampling rate. Acceleration level and erosion current increase sharply with the initial increase of gas content. The low amplitude of impact intensity at low gas content should be attributed to the delay and smaller volume of expanding vortex. Surprisingly the maximum of erosion occurs at lower gas content than the maximum of acceleration. This behavior is not completely understood yet and could be related to the position or the final size of the collapse on the exposed surface. In this case as shown on figure 14 the relation between acceleration and erosion rate is not unique. More tests are needed to clarify this.

The maximum erosion current of 0.04 μA corresponds, according to the jet calibration curve, to a very low erosion rate of 1.3 μg/h of titanium grade 1 or 4.2 μg/h of Al6061T6. Since there is 12000 impacts per hour, each impact removes on the average only 0.1 ng of titanium. These numbers illustrate the incredible sensitivity of the DECER technique used in the pulse mode.

Pit counting

Samples of Cu39 and 316L were impacted for 120 s, 400 collapses, at the three test conditions shown in table 4, except for Cu39 at the highest intensity for which the time was reduced to 45 s in order to avoid indentation overlap. The surfaces were scanned with the laser profilometer over an area of 2.2 mm by 2.2 mm. The total pitted area measured at different depths below the surface is shown on figures 15 and 16. The maximum pit depth for the most intense conditions of the vortex appears to be comparable to that of the least intense conditions of the jet at 6.9 MPa seen on figures 5 and 6, that is about 5 μm for Cu39 and

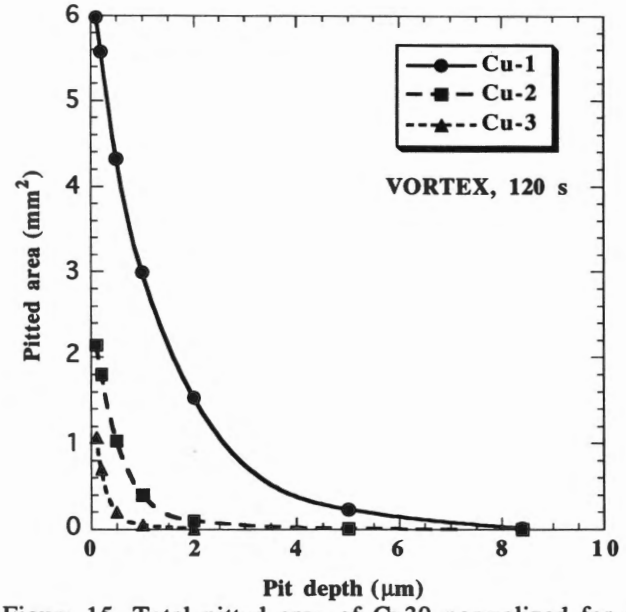

Figure 15. Total pitted area of Cu39 normalized for an exposure time of 120 s at the three vortex conditions.

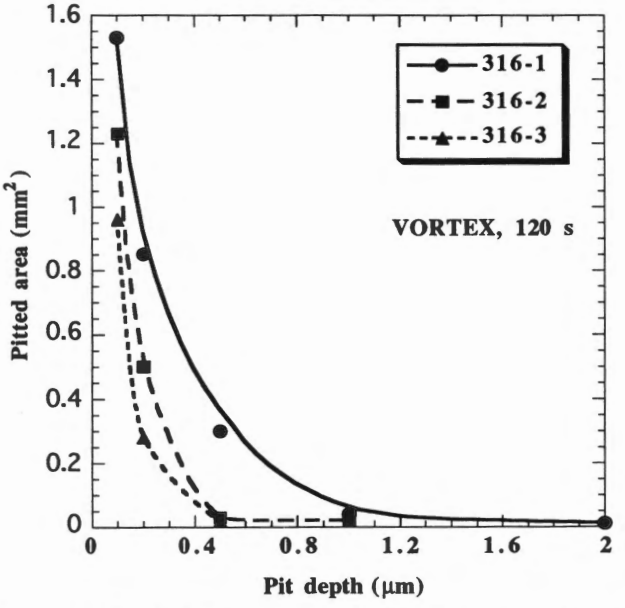

Figure 16. Total pitted area of 316L for an exposure time of 120 s at the three vortex conditions.

about 1 μm for 316L. Since the repetition rate of these impacts is more than 2 orders of magnitude less the volume pitting rate is also much smaller than on the jet as they will be compared below.

Vibration data

Figure 17 presents the inferred force in the 0.5 - 12 kHz bandwidth measured on the six different metal samples at the three vortex conditions. Most of the inferred forces were concentrated in that bandwidth. The inferred forces do not show a correlation with the metal hardness as in the jet

experiments. They all correlate well however with cavitation intensity.

On figure 18 we compare the correlations between weight loss and pitting rate against inferred force on 316L in both jet and vortex cavitation. The DECER erosion rate measured on the vortex on Ti1 was converted to Al6061T6 weight loss with jet weight loss data indicating an erosion rate ratio Al6061T6/Ti1 of 3.1. We see that the volume pitting rate and the inferred forces are more than two orders of magnitude lower in the vortex than in the jet. This is a direct measure of the much lower erosive power of the vortex. The pitting rates of Cu39 and 316L appear to fit well with the inferred force on more than 6 orders of magnitude. The weight loss rate in the vortex deduced from the DECER current appears to be too small to fit with the other data, probably because of incomplete incubation of the titanium probe surface. More erosion measurements are needed on the vortex.

CONCLUSION

The sensitivity of DECER electrochemical cavitation detection technique can be greatly improved by the use of the softest and purest grade of titanium now available 99.999 %. When used in the pulse mode for isolated cavitation impacts separated in time by more than 0.1 s it can detect metal losses as low as ng and erosion rates from 10^3 down to 10^{-3} mg/h with 1 cm^2 sensors.

The pit counting technique covers an even larger range of cavitation intensity when metals of different hardness are used. The softest Al 99.999 % appears more adapted for the lowest jet and vortex cavitation intensities. Pure copper and 316L stainless steel pitted surfaces yield a good measure of cavitation intensity for the full range of jet and vortex cavitation as indicated by the correlation with metal losses and acceleration data. The measured volume pitting rate for the more brittle alloys is smaller than their volume loss rate deduced from weight loss data. But it is larger for the more ductile and tougher metals such as Cu39 and 316L s. s.. The prediction of erosion rate from the pitting rate for a given material would require to take into account additional intrinsic properties such as resilience and fatigue resistance. The maximum depth of pits indicate that the vortex impact intensity is comparable to the jet impact intensity at the lowest pressure of 6.9 MPa. The measured pitted areas of different hardness metals provide a good way to map on an exposed surface the maximum stresses produced by cavitation.

The vibratory forces inferred from high frequency accelerometer data correlate well with volume pitting and loss rates in both vortex and jet cavitation over more than 6 orders of magnitude. For this technique also the nature and hardness of the impacted metal surface have an important effect.

These three techniques should be useful in characterizing the very low erosive power of turbine models.

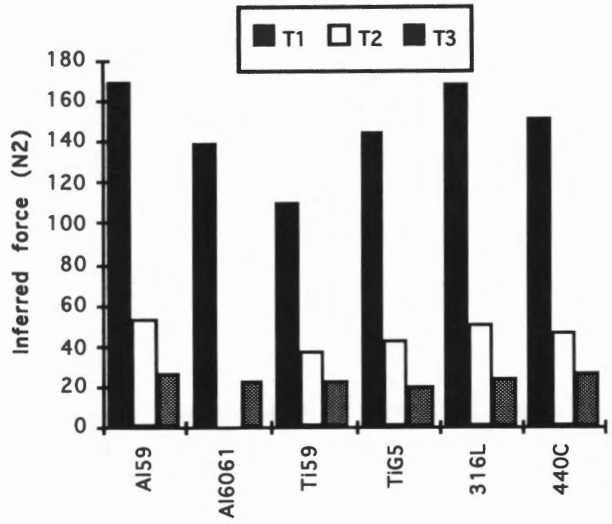

Figure 17. Inferred force (0.5-12 kHz) measured on the 6 metal sample at the 3 vortex conditions.

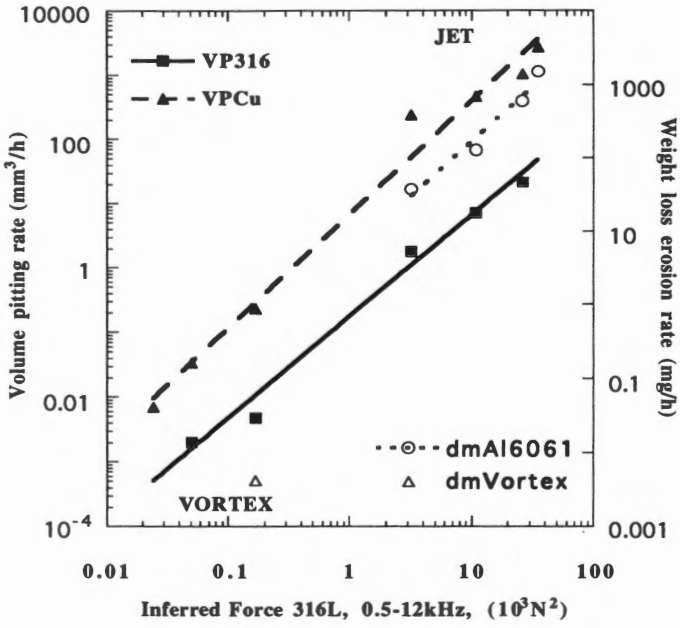

Figure 18. Correlation between the MSV of inferred force, the weight loss rate and the volume pitting rate of Cu39 and 316L in both jet and vortex cavitation.

ACKNOWLEDGMENT

The authors are grateful to Jacques Larouche and Pierre Lavigne of IREQ for their meticulous experimental work in the laboratory.

REFERENCES

1 Bourdon, P., Simoneau, R., Lavigne, P., "A vibratory approach to the detection of erosive cavitation", Proc. of Third International Symposium on Cavitation Noise and Erosion in Fluid System, ASME, December 1989, San Francisco (USA).

2 Abbot, P.A., "Cavitation detection measurements on Francis and Kaplan Hydroturbines", Proc. of Third International Symposium on Cavitation Noise and Erosion in Fluid System, ASME, December 1989, San Francisco (USA).

3 Lecoffre, Y., Marcoz, J., Franc, J. P., Michel, J. M., "Tentative procedure for scaling cavitation damage", Proc. Intern. Sympos. on Cavitation in Hydraulic Structure and Turbomachinery, ASME, June 1985, Albuquerque.

4 Belahadji, B., Franc, J. P., Michel, J. M., "A Statistical Analysis of Cavitation Erosion Pits", Journal of Fluids Engineering, Vol. 113, 1991, pp. 700 - 706.

5 Simoneau, R., Fihey, J.L., Chincholle, L.,"Effet d'Activation Anodique de la Cavitation Érosive", Proc. 11th IARH Symposium , September 1982, Amsterdam (NL)

6 Simoneau, R., Désy, N., Grenier, R., "Electrochemical detection of cavitation erosion on a pump-turbine model", Proc. 13th IAHR Symposium, September 1986, Montréal (Canada).

7 Simoneau, R., Avellan, F., Kuhn de Chizelle, Y., "On line measurement of cavitation erosion rate on a 2D NACA profile" Proc. of Third International Symposium on Cavitation Noise and Erosion in Fluid System, ASME, December 1989, San Francisco (USA).

8 Bourdon, P., Simoneau, R., Avellan, F., Farhat, M., "Vibratory characteristics of erosive cavitation vortices downstream of a fixed leading edge cavity", Proc. 15th IARH Symposium, 11-14 September 1990, Belgrade (Yugoslavia).

9 Bourdon, P., Simoneau, R., Désy, N., Do, N., Grenier, R., "Solving a Severe Cavitation Erosion Problem on a 50 MW Francis Turbine.", Proc. 14th IARH Symposium, 20-23 June, 1988, Trondheim (Norway)

10 Avellan, F., Farhat, M. "Shock Pressure Generated by Cavitation Vortex" Proc. of Third International Symposium on Cavitation Noise and Erosion in Fluid System, ASME, December 1989, San Francisco (USA).

FED-Vol. 176, Bubble Noise and Cavitation Erosion
in Fluid Systems
ASME 1993

CAVITATION EROSION INCEPTION AT HIGH HYDROSTATIC PRESSURES

G. Iernetti and P. Ciuti
Department of Physics
University of Trieste
Trieste, Italy

A. Francescutto
Dept. of Naval Architecture
University of Trieste
Trieste, Italy

N. V. Dezhkunov
Institute of Applied Physics
Minsk, Russia

M. Reali
ENEL–DSR–CRIS
Milan, Italy

ABSTRACT

The mass loss rate on aluminum foils due to vibratory cavitation in water and NaCl-water solutions and the sonoluminescence emission intensity have been measured for different values of the hydrostatic pressure ranging from 1 atm to about 12 atm. The specimen, an aluminum foil 13 μm thick, has been subjected to the action of a 24.1 kHz ultrasonic field. Varying the pressure amplitude through the adjustment of the transducer vibration amplitude, the incipient thresholds for the onset of both phenomena have been measured. The results indicate that by increasing the hydrostatic pressure both the mass loss rate and the sonoluminescence intensity pass through a maximum value several times greater than the value obtained at atmospheric pressure and then quickly decreases to zero.

The marked correlation between the thresholds of the two phenomena and between their intensities confirms the possibility of using sonoluminescence as a monitor of erosion.

INTRODUCTION

Recent research in cavitation erosion has been mainly aimed at discovering the correlations with other macroscopic phenomena to be used as efficient monitors of the inception and intensity of erosion (Lush, 1986, ITTC, 1987 and 1990). The first step consisted in the adoption of an efficient descriptor of the erosion intensity. To this end, cumulative mass loss, mass loss rate, erosion 'intensity', erosion 'strength', mean depth penetration rate and surface density of pits have been progressively introduced.
Then, the correlations were searched between the erosion intensity and the characteristics of the fluid flow, where applicable, or with other phenomena characteristic of cavitation, i.e. noise (global or spectral components), electrochemical current intensity and sonoluminescence intensity.

Many studies have been devoted to the use of noise as a monitor of erosion. This was suggested by the ease of noise measurements at different testing conditions and to the unwanted effects produced by noise itself, especially in ship propulsion.

As regards the use of electrochemical current, which is the basis for the DECER cavitation detector, some experimental results [4] indicate that the electrochemical potential difference during cavitation is one order of magnitude larger than the potential difference excited by the ultrasound only.

Only a few studies refer to the use of sonoluminescence. Among these, Van der Meulen (1986) concludes that further research is needed to clarify the correlation between sonoluminescence and erosion intensities. Acoustic signals or sonoluminescence correlate in fact with the collapse intensity of cavitation bubbles, but not always with the severity of erosion.

This paper concerns experiments performed in a vibratory cavitation rig where a stationary aluminum specimen is subjected to an ultrasonic beam. Aluminum has been chosen since this metal has often been considered with interest in the cavitation erosion literature. With a mind also to underwater applications, the tests have been conducted with hydrostatic pressure as a parameter.

EXPERIMENTAL SETUP AND RESULTS

The plane ultrasound transducer has a frequency of 24.1 kHz and the disk end of its wave guide has a diameter

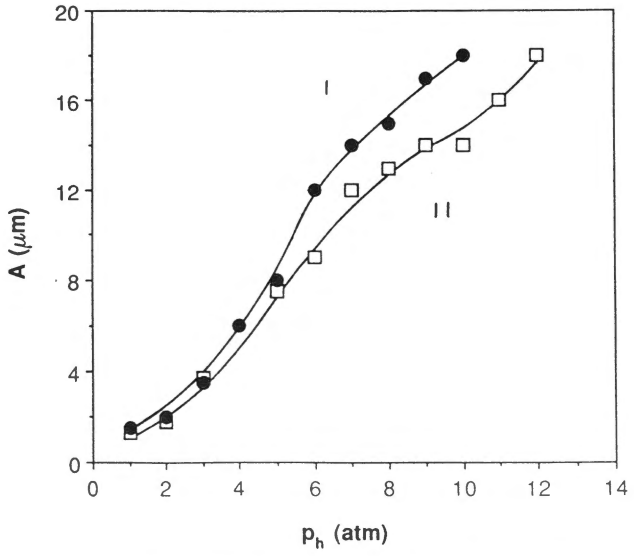

Fig. 1. Transducer amplitude thresholds for erosion (curve I) and sonoluminescence (curve II) in distilled water after three days of standing in the cell.

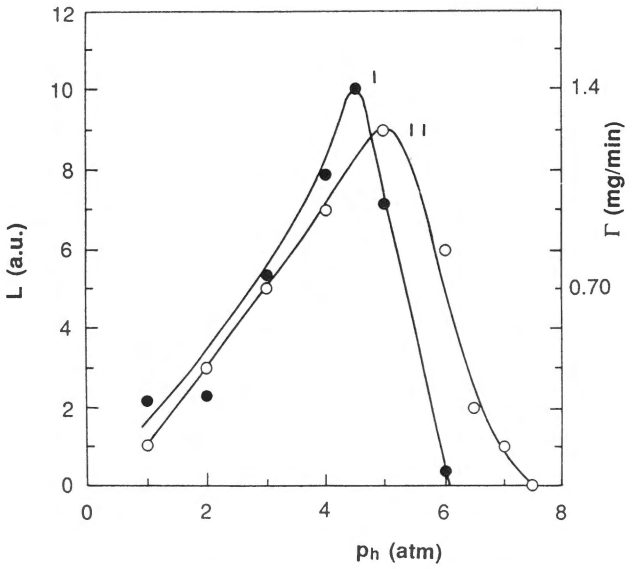

Fig. 2. Erosion rate Γ and sonoluminescence intensity L, for transducer amplitude A=12μm, as a function of the hydrostatic pressure for distilled water after three days of rest in the cell:
- curve I erosion rate Γ (mg/min);
- curve II sonoluminescence intensity L (a.u.).

of 15 mm. It was mounted in the high pressure cell (Fanelli and Reali, 1985), which has a manometer and a transparent window seen by a photomultiplier (see Dezhkunov et al., 1993 for further details). Aluminum foils (98.89%) 30 mm x 40 mm size and 13 μm thickness were used as erosion test samples. Each foil was placed in a plane perpendicular to the ultrasound beam axis at a distance d = 20 mm from the disk end of the sound wave guide. The weight loss ΔG of the specimen, measured in each experiment, was carried out under conditions of continuous irradiation.

The thresholds of sonoluminescence emission and of erosion inception have been measured as a function of hydrostatic pressure p_h. Pressures higher than atmospheric pressure have been obtained with hydraulic pressurization rather than by gas pressurization. This has important consequencies on the gas content of the liquid at high pressures. The threshold values of the transducer's vibration amplitude A, as a function of p_h, are given in Fig. 1 in distilled water which was kept three days standing in the cell. Curve I refers to erosion, curve II to sonoluminescence. The threshold for erosion is a little higher than the one corresponding to light emission.

Typical results indicate that the erosion rate $\Gamma = \Delta G/t_s$ (indicated often in the literature as MLR or mass loss rate) shows a time behaviour characterized by an initial linear acceleration phase, followed by a deceleration phase. This means that, in the acceleration phase, the mass loss ΔG is roughly quadratic with time. This has been observed in our experiments (Dezhkunov et al., 1993) for the interval preceding the plateau. The presence of a plateau in our case is mainly attributable to geometric effects of the aluminum surface and to the small thickness of the sample rather than to the effect of the deceleration phase, which is not observed with thin specimens. The first part (1-2 min) of the acceleration phase of the curves is approximately linear and is used for the following measurements.

The dependences of the erosion rate Γ (curve I) and of the sonoluminescence intensity L (curve II) on p_h is shown in Fig. 2, together with the erosion rate dependence on p_h in a sample of water with low content of nuclei and bubbles. The erosion rate (curve I) and the sonoluminescence intensity (curve II) correspond to the same bubble content. Both L and Γ increase, achieve a maximum and then decrease. As regards the sonoluminescence, its behaviour, as a function of hydrostatic pressure, is in accordance with the results of Finch and Chendke and Fogler reported in (Walton and Reynolds, 1984). The dependences of L and Γ on p_h are given in Fig. 3 for a NaCl water solution (concentration 70 g/ dm^3). The dependences of L and of Γ on p_h are rather similar between themselves indicating a strong correlation between the two phenomena.

DISCUSSION AND CONCLUSIONS

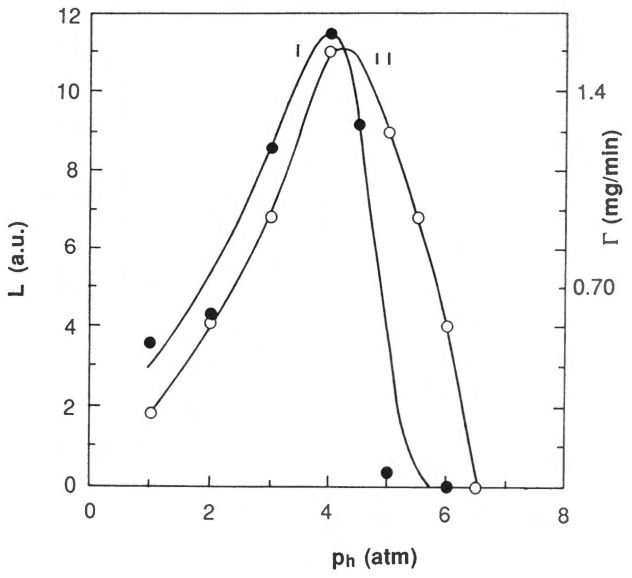

Fig. 3 Erosion rate Γ and sonoluminescence intensity L, for transducer amplitude A = 12 μm, as a function of the hydrostatic pressure in NaCl water solution:
- curve I erosion rate Γ (mg/min) in NaCl-water solution; (concentration c = 70 g/dm^3) and three days of rest in the cell ;
- curve II sonoluminescence intensity L (a.u.) in NaCl-water solution. Same conditions as for curve I.

The effect of hydrostatic pressure on the nuclei and bubble population and on the acoustic cavitation threshold for a single bubble is discussed in (Dezhkunov et al., 1993). Shortly, the increase of p_h by means of hydrostatic pressurization reduces the gas saturation of the liquid. The acoustic energy available per collapsing bubble increases, increasing the yield of light and erosion. A further increase of pressure reduces too much the bubble population in the range of radii explored by the acoustic field, thus producing a sharp decrease of sonoluminescence and erosion. This is in agreement with the curve representing the incipient threshold shown in Fig. 1.
for a single bubble is discussed in (Dezhkunov et al., 1993). Shortly, the increase of p_h by means of hydrostatic pressurization reduces the gas saturation of the liquid. The acoustic energy available per collapsing bubble increases, increasing the yield of light and erosion. A further increase of pressure reduces too much the bubble population in the range of radii explored by the acoustic field, thus producing a sharp decrease of sonoluminescence and erosion. This is in agreement with the curve representing the incipient threshold shown in Fig. 1.

The light emission and the erosion activity in the NaCl water solution (curve I and curve II of Fig. 3) show both a higher maximum and lower p_h values of desinence than the corresponding values of curve I and II of Fig. 2. Indeed, the NaCl water solution has nuclei and bubbles contents smaller than the one present in distilled water after three days of rest. The above data agree with previous results at atmospheric pressure (Ciuti et al., 1987, Dezhkunov et al., 1986).

The good correlation between the erosion rate and the sonoluminescence intensity suggests that the two effects are based on the same process namely bubble oscillation and collapse. The fact that the vibration amplitude threshold is higher for erosion than for sonoluminescence may be explained by the two following considerations:
- the light emission is given both by stable (Lush, 1986, ITTC, 1987) and by transient bubbles. The erosion is given only by transient bubbles imploding at or near the specimen surface;
- the light emission takes place also in proximity of the transducer where the ultrasound intensity is higher that that at the specimen surface.

The effect of the variation of nuclei and bubble content on the thresholds and on the intensities of sonoluminescence and mass loss, is now under study. Preliminary results relative to the sonoluminescence intensity only are reported in Dezhkunov et al. (1993). It appears that, by increasing nuclei and gas content, the intensity of the peak is reduced whereas the location of the maximum amplitude and the desinence are shifted towards higher values of p_h.

The following conclusions can be drawn from this study:

1. The present experimental results demonstrate the strong influence of ambient hydrostatic pressure on cavitation induced luminescence and erosion.
2. The strict correlation found for the dependence on p_h for both sonoluminescence and erosion could justify the use of sonoluminescence emission as a monitor of the appearance and of the intensity of erosion. Previous hydrodynamic tests (Van der Meulen, 1986) would thus be corroborated by the present vibratory tests.
3. It appears that it is very difficult to have erosion at an ambient pressure greater than about 10 atm in water.

ACKNOWLEDGMENTS

This research has been partially supported by:
- ENEL, by the contract ENEL-Department of Physics of Trieste University;
- MURST, for the research: Physicochemical mechanisms of cavitation effects;
- Fund for Fundamental Researches of Republic Belarus, C S I.

REFERENCES

Ciuti, P., Francescutto, A., Iernetti, G., and Dezhkunov, N.V., 1987, "Acoustic Cavitation in NaCl Water Solutions", *Proceedings, 11th International Symposium on Nonlinear Acoustics*, V.K. Kedrinskii, ed, Novosibirsk, Part I, pp. 27-31.

Dezhkunov, N., Iernetti, G., Prokhorenko, P.P., Francescutto, A., and Ciuti, P., 1986, "Sonoluminescence and Subharmonic Generation in a Cavitation Zone of Aqueous Sodium Chloride Solutions", *Journal of Engineering Physics*, Vol. 51, pp. 1052-1058.

Dezhkunov, N. V., Francescutto, A., Iernetti, G., 1990, "Electrochemical Potential Difference Generated by Cavitation", *Proceedings, 19th International Towing Tank Conference*, Madrid, Vol. 2, pp. 87-88.

Dezhkunov, N. V., Iernetti, G., Francescutto, A., Reali, M., Ciuti, P., 1993, "Cavitation Erosion and Sonoluminescence at High Hydrostatic Pressures", Submitted to *Acustica*.

Fanelli, M., Reali, M., 1985, "A Pressure and Temperature Controlled Chamber for Studies of Gaseous-Vapor Nucleation and Bubble Dynamics in Water and other Liquids", *Proceedings, 7th International Symposium on Water Column Separation*, M. Henriksson, ed, Älvkarleby, pp. 4.1-4.6.

Gaitan, D.F., Crum, L.A., Church, C.C., Roy, R.A., 1992, "Sonoluminescence and Bubble Dynamics for a Single, Stable, Cavitation Bubble", *Journal of Acoustical Society of America*, Vol. 91, 3166-3183.

ITTC, 1987, Report of the Cavitation Committee, *Proceedings, 18th International Towing Tank Conference*, Kobe, Vol. 1, pp. 159-220.

ITTC, 1990, Report of the Cavitation Committee, *Proceedings 19th International Towing Tank Conference*, Madrid, Vol. 1, pp. 161-233.

Lush, P. A., 1986, "Some Advances in Cavitation Erosion and Noise Research", *Proceedings, International Symposium on Cavitation*, H. Murai, ed, Sendai, pp. 317-322.

Van der Meulen, J.H.J., 1986, "On Correlating Erosion and Luminescence from Cavitation on a Hydrofoil", *Proceedings, International Symposium on Propellers and Cavitation*, The Editorial Office of Shipbuilding of China, Wuxi, pp. 261-270.

Walton, A. J. and Reynolds, G. T., 1984, " Sonoluminescence ", *Advances in Physics*, Vol. 33, pp. 595-659.